Proceedings of the
Annual Stability Conference
Structural Stability Research Council
San Antonio, Texas, March 19-22, 2024

Computational and experimental comparison on stability behavior of the cold-formed steel diaphragm sheathed with oriented strand boards

Sheila Ariana[1], Hernan Castaneda[2], Kara D. Peterman[3]

Abstract
Lightweight frames are susceptible to lateral loads in terms of stability behavior. To mitigate this problem, frames are sheathed with various sheathing materials. Previously, the cantilever cold-formed steel diaphragm sheathed with oriented strand boards (OSBs) were experimentally tested at the University of Massachusetts Amherst. In this study, a high-fidelity model is developed to simulate this system, and the results of the computational and experimental test, including strength and structural stability, are compared and discussed. The system is a 10 ft. by 15 ft. diaphragm consisting of two ledgers connecting to one another with 8 equally spaced joists. Ledgers and joists are fastened via clip angles, and the steel frame is sheathed with oriented strand boards. The computational model is capable of capturing system strength, load path, failure of the connections, and stability to the extent to which local lip buckling and lateral torsional buckling of the joists of the CFS frame and separation of the sheathing panels due to their movement during loading are observed. Stability issues of the diaphragm sheathed with the OSBs are distributed in various elements of the frame. The strength of the system manifests the reflection of these stability issues. Numerical results including shear strength, connection failures and stability response closely align with the experimental test. These constant efforts are taken to shed light on the complex load transfer mechanism and stability of the cold-formed steel diaphragms.

1. Introduction and outline

In a conventional configuration, a cold-formed steel floor diaphragm is composed of a structural framework, including CFS floor joists which are uniformly distributed. These joists are attached to the ledgers and overlaid with various structural panels such as plywood, oriented strand boards, corrugated steel decks, fiber cement boards to augment the lateral resistance and thereby enhancing the overall performance of the diaphragm (S. Zhang & Xu, 2018).

Diaphragm can generally be classified as flexible, rigid, or semi-rigid when subjected to a comparative analysis of the maximum deflection and the average inter-story drift. This classification plays a crucial role in the study and understanding of structural behavior (American Society of Civil Engineers (ASCE 7-16), 2016).

[1] PhD Candidate and Graduate Research Assistant, University of Massachusetts Amherst, <sariana@umass.edu>
[2] PhD, Project Consultant, Simpson Gumpertz & Heger (SGH), <hcastaneda@sgh.com>
[3] Associate Professor, University of Massachusetts Amherst, < kdpeterman@umass.edu >

The CFS-NEES project conducted by Peterman, demonstrates that CFS diaphragms exhibited characteristics of semi-rigid diaphragms, leaning more towards rigid diaphragms. This behavior was observed even though they were designed as flexible diaphragms, adhering to the current design code. In this full-scale experimental test, the contribution of the nonstructural elements on the lateral response of the CFS-framed building with OSB-sheathed shear walls is explored. ((Peterman et al., 2016) and (Peterman et al., 2016)).

The experimental predictions conducted by Nguyen (Nguyen et al., 1996), Serrette (Reynaud Serrette et al., 2007), and Morgan (Morgan et al., 2002) on the lateral strength of the CFS shear walls sheathed with Oriented Strand Board (OSB) provides a scientific basis for understanding the structural behavior of the shear walls. This basis was adopted in the current standard design provisions in North America. Many researchers at McGill University ((Zhao, 2004), (Blais, 2007), (Branston et al., 2006), (Boudreault et al., 2007)) investigated the lateral response of the CFS shear walls sheathed with Oriented Strand Board (OSB) and plywood.

In an experimental study performed by Yu in 2010 the impact of the several factors, including the aspect ratio of the wall, the thickness of the steel sheet and the fastener spacing of the sheathing connections, were explored on the behavior of the shear walls sheathed with steel sheets (Yu, 2010). In addition, Fülöp and Dubina (Fülöp & Dubina, 2004) and Zhang et al. (W. Zhang et al., 2017) examined the behavior of the shear walls sheathed with steel deck under lateral and gravity loading.

Utilization of the Fiber-Cement boards (Ariana & Peterman, 2023), (Ariana & Peterman, 2022) and gypsum sheathings in the experimental tests results in the higher strength of the system (Mohebbi et al., 2016).

The experimental tests conducted by Nikolaidou concluded that the application of fasteners throughout the entire boundary of the panels, a technique referred to as a ‘blocked diaphragm’, results in a substantial enhancement of the strength of the diaphragm. The behavior of the screw connections is dependent on the screw size. As the diameter of the screw increases, the failure mode transitions from screw shearing to wood bearing (Nikolaidou & Latreille, 2016).

Based on AISI-S907, all current analytical techniques for diaphragms rely on a system effect. This effect encompasses the combined influence and interaction of the sheathing panels, support and sidelap connections in the generation of shear strength and stiffness per unit length. The failure modes of the diaphragms are predominantly connection-centric or are confined by the out-of-plane buckling of the diaphragms. This underscores the pivotal role of connection robustness and structural stability in the overall performance of the diaphragms (American Iron and Steel Institute (AISI S907), 2017).

In a study on a wood-sheathed CFS framed diaphragm, a computational model was developed by Chatterjee et al. (Chatterjee et al., 2017) using ABAQUS, which depicted a non-linear finite element model (FEM) under both monotonic and cyclic loading. The model successfully replicated the peak strength observed in the experimental results; however, it encountered challenges in accurately capturing the response post the peak load.

Filiatrault formulated a numerical model that evaluates the non-linear response of wood framed shear walls with varying dimensions and frame-to-sheathing connectors under static lateral loads (Filiatrault et al., 2002), and arbitrary quasi-cyclic loading (Bryan Folz & Filiatrault, 2001). The model is capable of predicting the lateral stiffness, the ultimate lateral load carrying capacity and the dynamic response. This research finding highlights that the intricate interaction between individual fasteners and the sheathing plays a crucial role in comprehending the non-linear behavior of the entire shear wall. The relative motion between the sheathing and framing results in the fasteners progressively damaging the sheathing panels, which in turn leads to a non-linear response.

In a numerical fastener-based model of a CFS shear wall developed by Tun in OpenSees, the ledger web, assumed as rigid, increases the initial stiffness of the shear wall marginally, and the non-linear strength of the system surpassed the result of the experimental tests significantly. The model incorporated every individual fastener, enabling a detailed examination of the interaction forces between the fasteners, framing elements and sheathing panels (Hein Tun, 2014).

In the computational simulation to validate the result of the experimental tests in OpenSees, the fastener-based numerical model of the wood-sheathed CFS shear walls demonstrated a reasonable replication of the force-displacement hysteretic response. When compared to the specification-based strengths, the computational models predicted 14% and 33% increase in the strength and drift at failure respectively (Buonopane et al., 2015).

In this study, a high fidelity finite element model is developed to corroborate the findings of an OSB-sheathed diaphragm test at the University of Massachusetts Amherst. The lateral response of the CFS-framed diaphragms were experimentally tested using the cantilever testing method, and are compared to the outcomes of the numerical simulation and the predictions based on the AISI S400 to confirm the system's strength, load transfer mechanism, and stability behavior. This work aims to shed light on the behavior of the CFS diaphragms sheathed with OSBs under lateral loads and serves as a supplement to a larger effort to develop seismic design of CFS structures.

2. Experimental Testing of the CFS-Framed Diaphragm Sheathed with OSBs

The frame of the diaphragm consists of two CFS ledgers connecting to each other via eight equally spaced CFS joists following the cantilever testing method. These joists attached to the ledgers with clip angles, fastened from each leg via six screws. The details of the geometry, test setup, dimensions of the CFS elements, connections and configuration of the frame in the test rig are presented in the paper comparing the progression of the failure in the experimental and numerical models of the CFS-framed diaphragm sheathed with steel deck (Ariana et al., 2023).

Table 1: Test Matrix of the CFS Diaphragm Components

Element	Dimensions (in)		Design Thickness (in)
Ledger (1200T200-54)	Web Depth	12 (304.8 mm)	0.0566 in (1.37 mm)
	Flange Width	2 (50.8 mm)	
Joist (1200S200-54)	Web Depth	12 (304.8 mm)	0.0566 in (1.37 mm)
	Flange Width	2 (50.8 mm)	
Clip Angle	Legs Width	3.5 (88.9 mm)	0.0566 in (1.37 mm)
	Length	11 (279.4 mm)	
Oriented Strand Board	Width	48 (1219.2 mm)	23/32 in (18.26 mm)

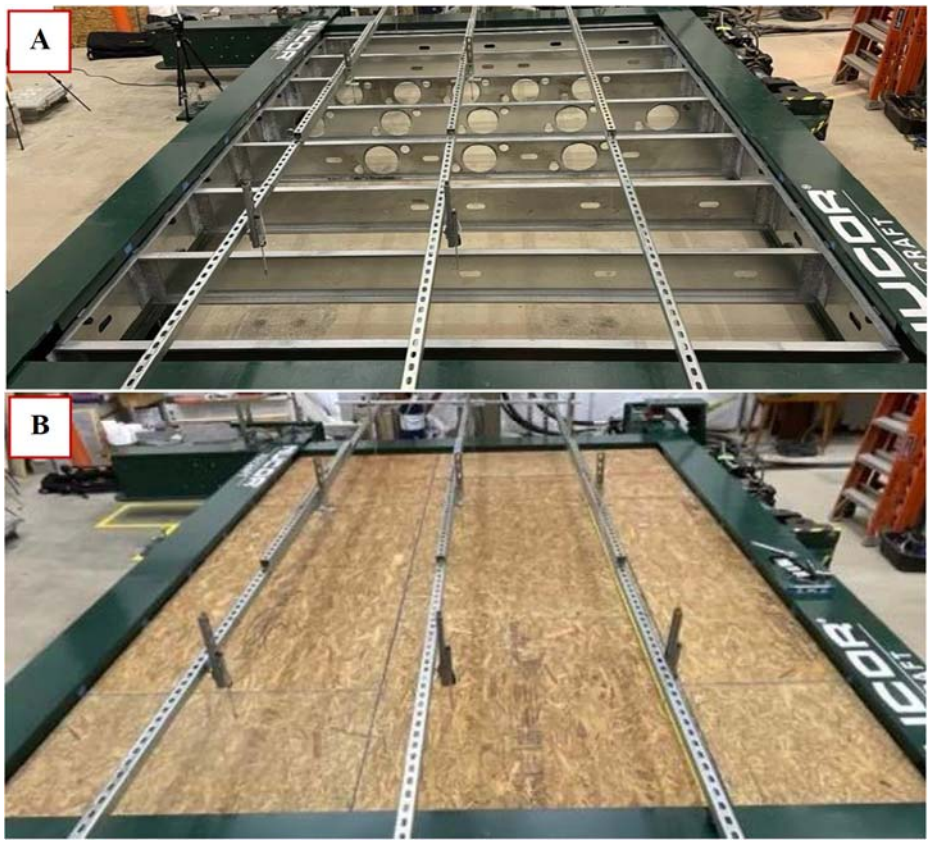

Figure 1: Images of the CFS-framed diaphragm: (A) before OSB installation – (B) after OSB installation

The test matrix of the diaphragm components is presented in Table 1. Fig. 1 shows the images of the tested diaphragm capped with OSBs.

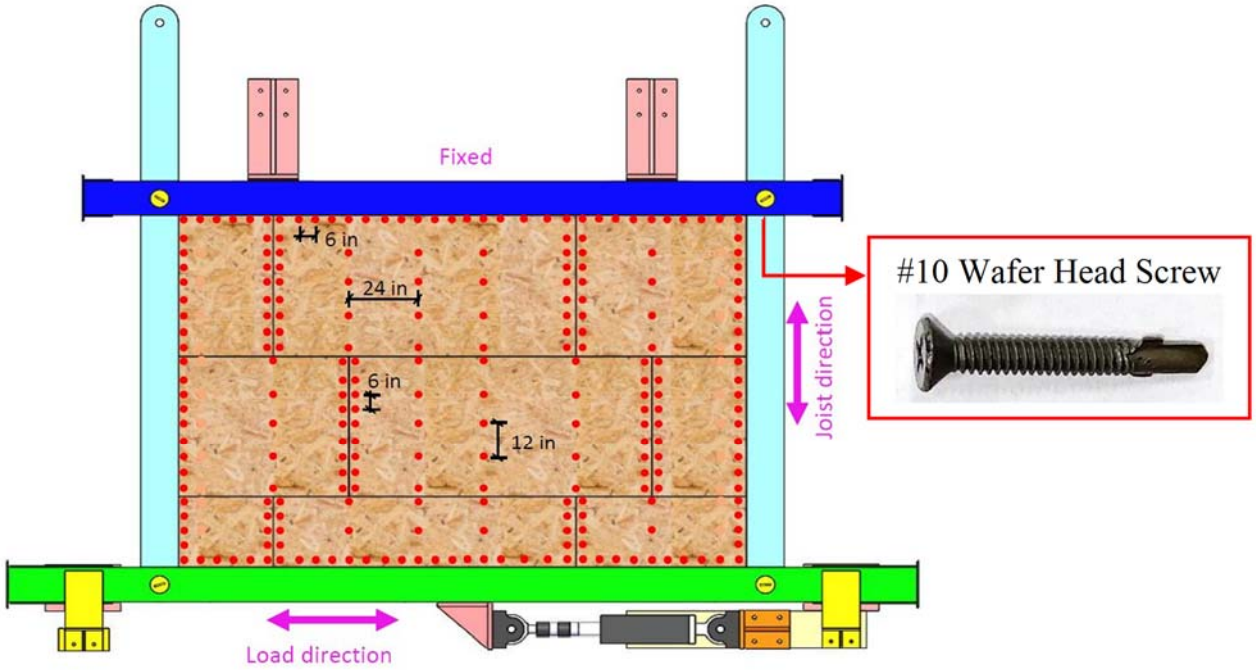

Figure 2: Images and location of the fasteners of the diaphragm sheathed with OSBs

The panels of the OSB-sheathed diaphragm are affixed to the frame using self-drilling #10 wafer head screws. Fig. 2 provides a visual representation and location of the fasteners.

The tests on the diaphragms are conducted using a displacement-controlled load, maintaining a steady load rate of 0.01 in/sec.

3. Finite Element Modelling of the CFS-Framed Diaphragm Sheathed OSBs

The system is represented as a three-dimensional shell using the ABAQUS software (Dassault System Simulia Corporation, 2014). The presented high-fidelity models are capable of capturing the lateral response of the diaphragm to the extent to which the stability behavior of the CFS frames including local and lateral torsional of the elements and progression of the failure of the connections can be explored.

3.1 Contact Interactions and Connections of the Finite Element Model

The geometrical and dimensional attributes of the ledgers, joists, clip angles and OSB are modeled in accordance with the elements utilized in the experimental test. The computational model incorporate four-node thin shell (S4R) elements for the parts of the computational model.

Steel is characterized as a homogeneous material with bi-linear elastic-perfectly-plastic properties. OSB is defined as an orthotropic material.

Numerical details of the model were previously presented in a study comparing the experimental and computational lateral response of this system sheathed with steel deck (Ariana et al., 2023).

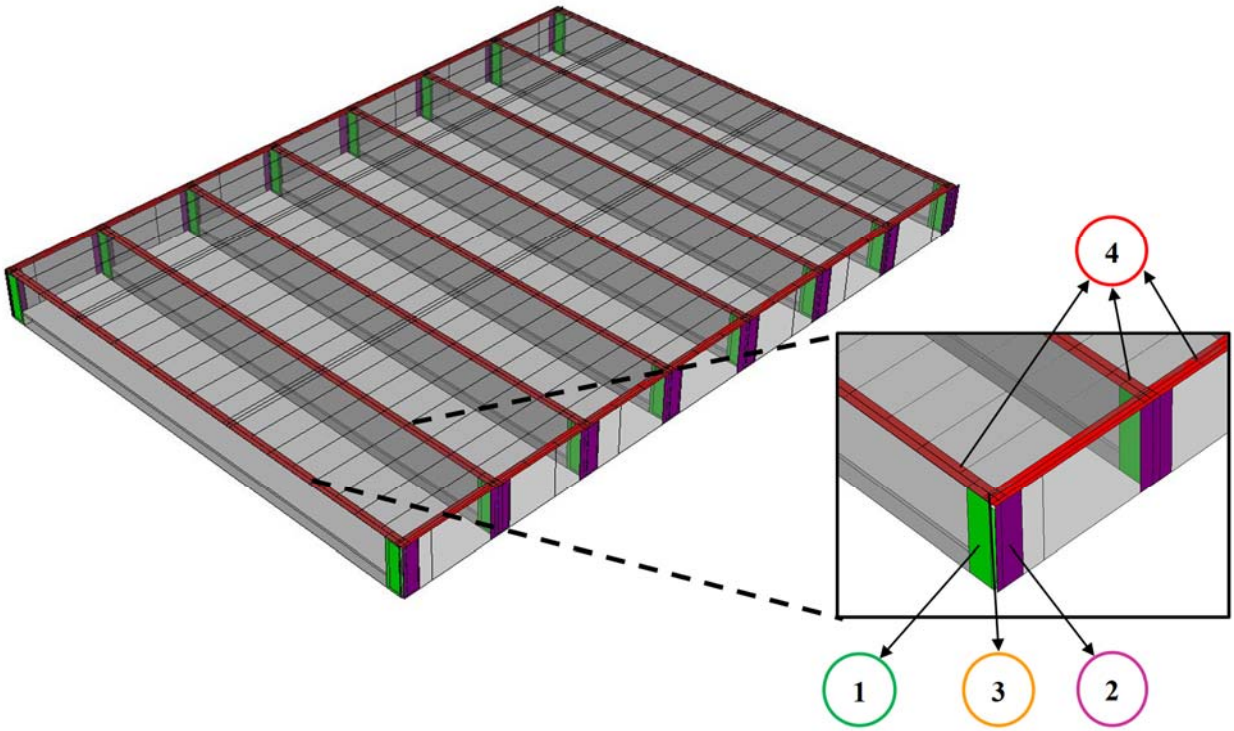

Figure 3: Contact pairs of the diaphragm models: (1) clip angle-to-joist – (2) clip angle-to-ledger – (3) ledger-to-joist – (4) OSB-to-joist and ledger

In the contact interactions, contacts are characterized as surface-to-surface. This formulation is applied to surfaces that are parallel to each other. Given that both surfaces can deform in the simulation, the more rigid one is selected as the master surface (Dassault System Simulia Corporation, 2014). The sliding formulation employs finite sliding, which permits possible sliding, rotation, and separation between the contact surfaces.

Fig. 3 depicts the pairs of the contacts of the OSB-sheathed diaphragm.

The interaction properties of each contact pair are characterized by two types of behavior: normal and tangential. For the normal behavior, a "Hard" contact is employed for the pressure-overclosure interaction, with non-linear behavior considered as the contact stiffness. As for the tangential behavior, a penalty formulation is used, with a friction coefficient set at 0.2.

Connections of the model are defined as wires exhibiting multi-linear elastic behavior to simplify the geometry and reduce the computational time of the model. This approach simulates the shear and pull-out behavior of the fasteners, taking into account local coordinates of the connectors.

The shear behavior of the connections is determined based on the load-displacement characterization of the connections derived from experimental work conducted at the Virginia Polytechnic Institute and State University ((Tao & Moen, 2017)). Due to a lack of data for the aforementioned connections, the pull-out behavior of the connection is defined as rigid.

3.2 Meshing of the Simulation

In the simulation of the diaphragm, elements are defined as 4-node thin shell elements. A quadrilateral mesh is structured using an approximate aspect ratio of 1:1.

In this paper, stability behavior of the systems is investigated. To this end, it is crucial for the model to capture buckling of the diaphragm.

A computational study performed by Schafer et al. concluded that a coarse mesh, while providing a rudimentary approximation to local buckling in finite element analysis, suffices for distortional and global modes. In contrast, medium and fine meshes are capable of accurately replicating all buckling modes (Schafer et al., 2010).

In this study, for parts of the elements where connections are absent, a medium mesh of 12 mm is specified. Conversely, a finer mesh of 6 mm is employed for regions in the vicinity of the connections.

3.3 Boundary Conditions, and Loading of the Simulation

Adhering to the cantilever testing method, one side of the frame is fixed, and the load is incrementally applied to the opposing side of the diaphragm. Fig. 4 depicts the boundary condition and the loading points on the numerical model.

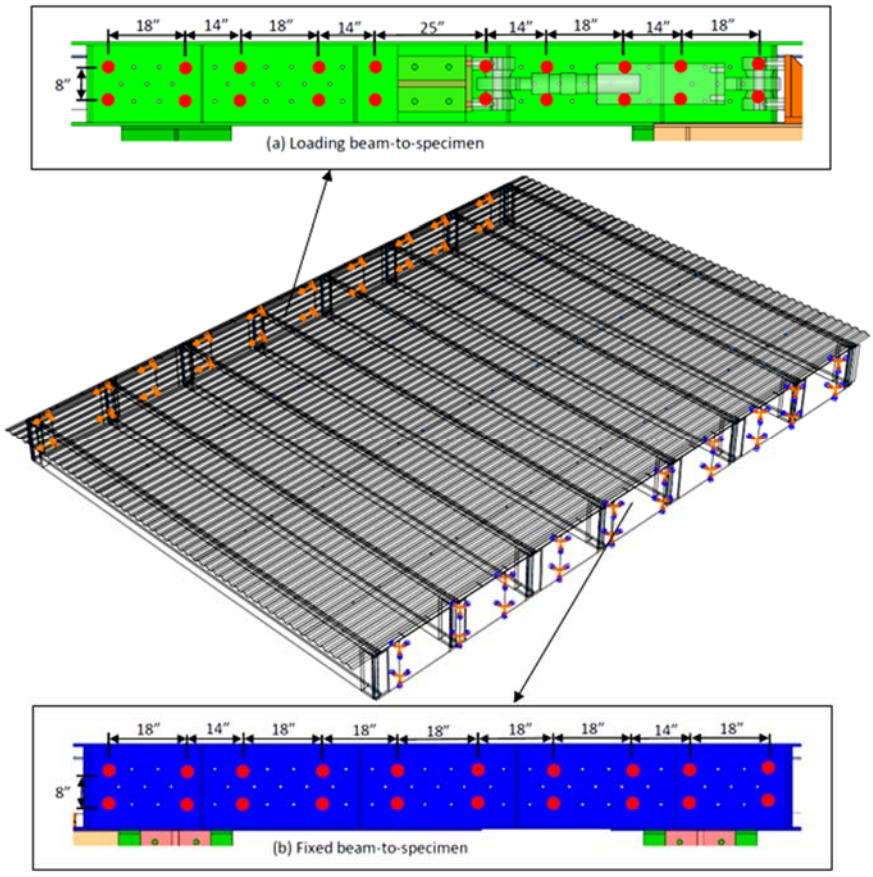

Figure 4: Boundary Conditions and Loading in the Simulated Diaphragm: (a) Loading Points on the Rig Frame – (b) Fixed Points on the Rig Frame

4. Prediction of the shear strength based on the code

Shear strength of the diaphragm sheathed with OSBs is derived from a linear interpolation of the nominal shear strength per unit length for diaphragms sheathed with wood structural panel sheathing provided by AISI S400 (American Iron and Steel Institute (AISI S400), 2015). This approach is necessitated due to the absence of shear strength values for OSB panels of 23/32 inches thickness in the AISI S400 provisions. The outcome of the interpolation process yields a shear strength value of 0.96 kips/ft.

5. Lateral response of the CFS diaphragm sheathed with OSBs

The lateral results of the diaphragms sheathed with OSBs are presented herein. The strength, stability response and the connection failure of the system are evaluated and discussed in the following sections.

5.1 Stability behavior of the system sheathed with OSB panels

Transmission of the load applied to the OSBs causes three different connection failure modes in the experimental test. OSB-to-CFS connections failed due to edge tear-out of the panels, pull-through or pull-out of the fasteners in the experimental test. With progression of failure in the sheathing-to-frame connections, the separation of the OSBs from the CFS frame is identified in the tension zone of the experiment and numerical simulation (Fig. 3). Consequently, higher load is transferred to the frame, causing two stability issues in the CFS-framed diaphragm. Local lip

buckling of the joists in the compression zone is identified as the first stability issue of the diaphragm sheathed with OSBs, and lateral torsional buckling in the joists is observed as the second stability problem of the system. These two stability issues are noticed in both experimental and computational models of the OSB-sheathed diaphragms and are shown in Fig. 4 and Fig. 5 respectively.

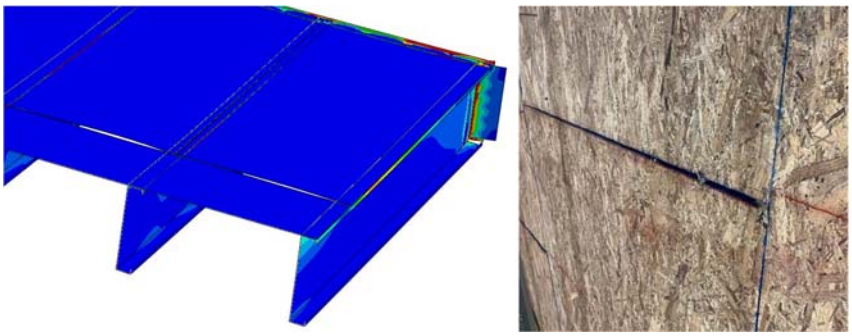

Figure 3: Separation of the OSBs in the CFS diaphragm in the both computational and experimental tests

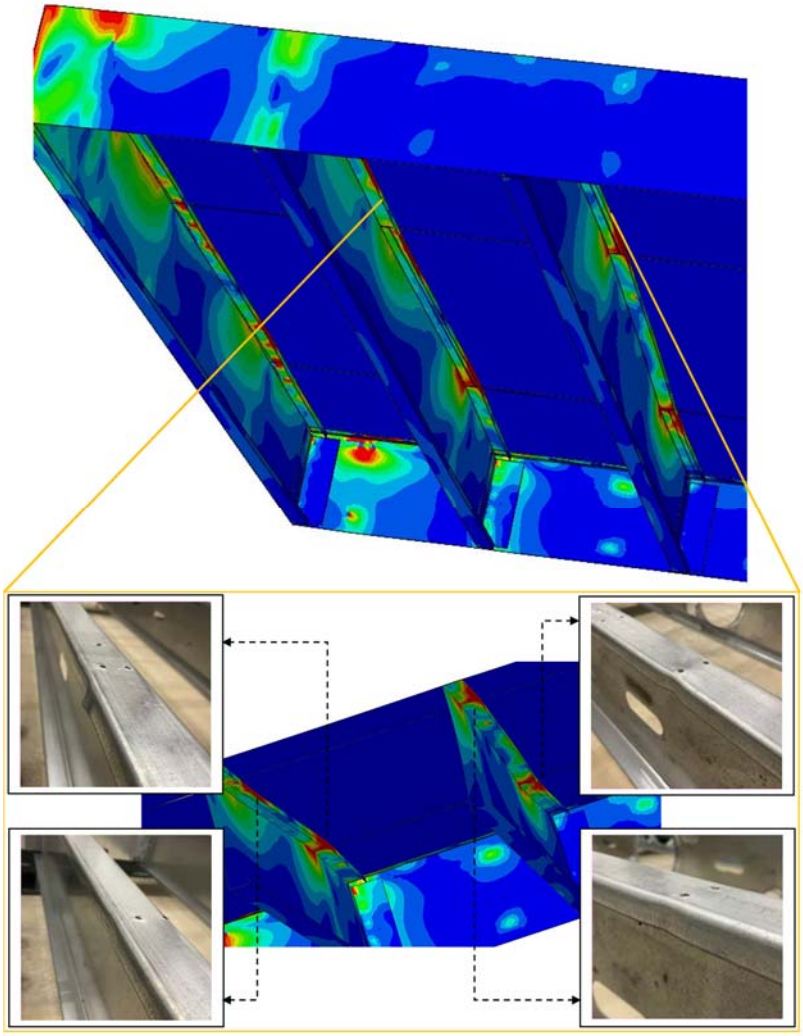

Figure 4: Local buckling of the upper lip of the CFS joists in the OSB-sheathed CFS diaphragm in the both computational and experimental tests

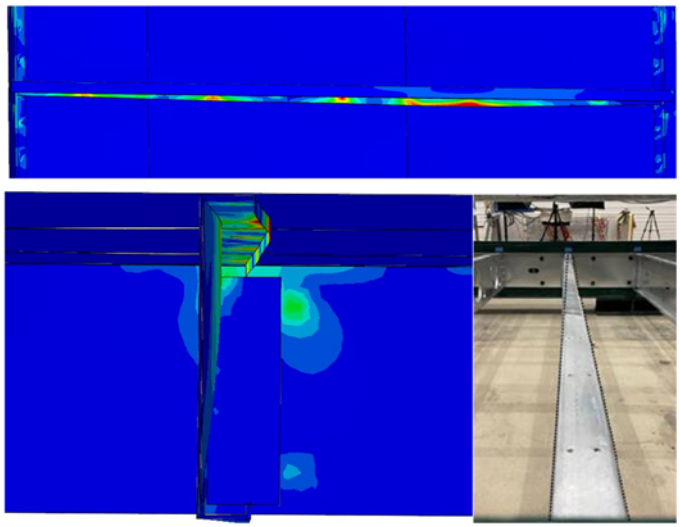

Figure 5: Lateral torsional buckling of the joists in the OSB-sheathed CFS diaphragm in the both computational and experimental tests

5.2 Shear strength of the system sheathed with OSB panels

The shear strengths derived from computational analysis, experimental tests and the equations suggested by AISI S400, (American Iron and Steel Institute (AISI S400), 2015), are plotted against the displacement of the CFS system in Fig. 6.A. This comparison is made to validate the results and assess the shear response of the system. Fig 6.B depicts the Von-Mises stress of the OSB-sheathed diaphragm.

The maximum shear strengths estimated based on the AISI S400 recommended table, the experimental test and numerical model are closely aligned. The AISI S400 predicts a maximum shear strength of 9.6 kips, while the computational and experimental tests lead to values of 9.91 and 10.03 kips, respectively. A minimal variability of 1% is observed between the peak strength of the OSB-sheathed diaphragm in the experimental and computational model. It is worth noting that the estimated strength of the diaphragm capped with OSBs is conservatively derived from a linear interpolation. This approach is necessitated due to the absence of strength values for 23/32 in thick OSBs in the AISI S400 provisions.

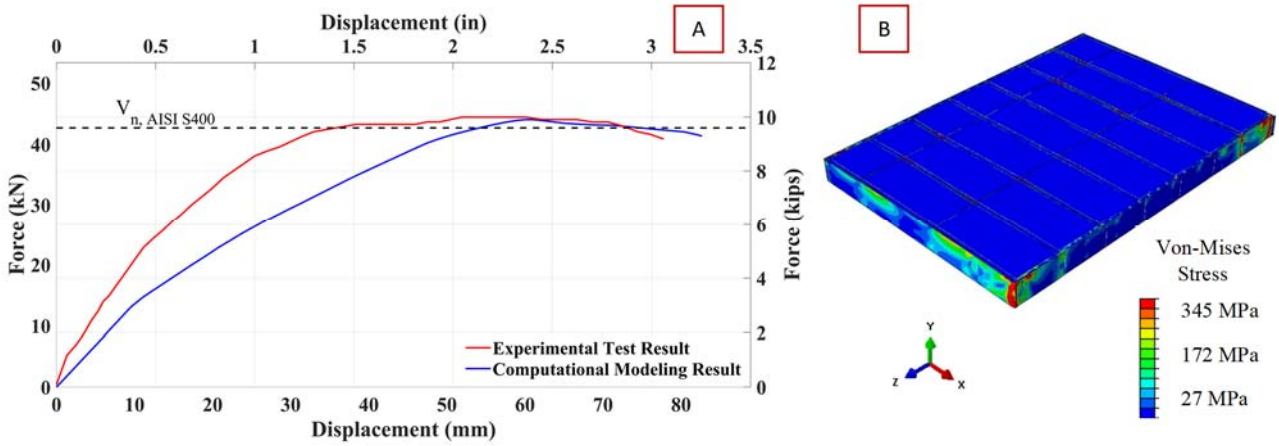

Figure 6: lateral response of the diaphragm: (A) Resultant shear strength of the OSB-sheathed CFS diaphragm (Force-Displacement curve) – (B) Von-Mises stress in the computational model

During the experimental test, the system's peak shear strength plateaus when the diaphragm's displacement ranges between 2.1 and 2.4 inches. This displacement at peak load is consistent with the 2.4 inches observed in the computational model, thereby validating the response of the CFS diaphragm sheathed with OSBs.

5.3 Failure of the fasteners in the diaphragm sheathed with OSB panels

In the experimental test, three distinct failure modes were identified as fastener pull-out, fastener pull-through, and panel edge tear-out (refer to Fig. 7.B, 7.C and 7.D).

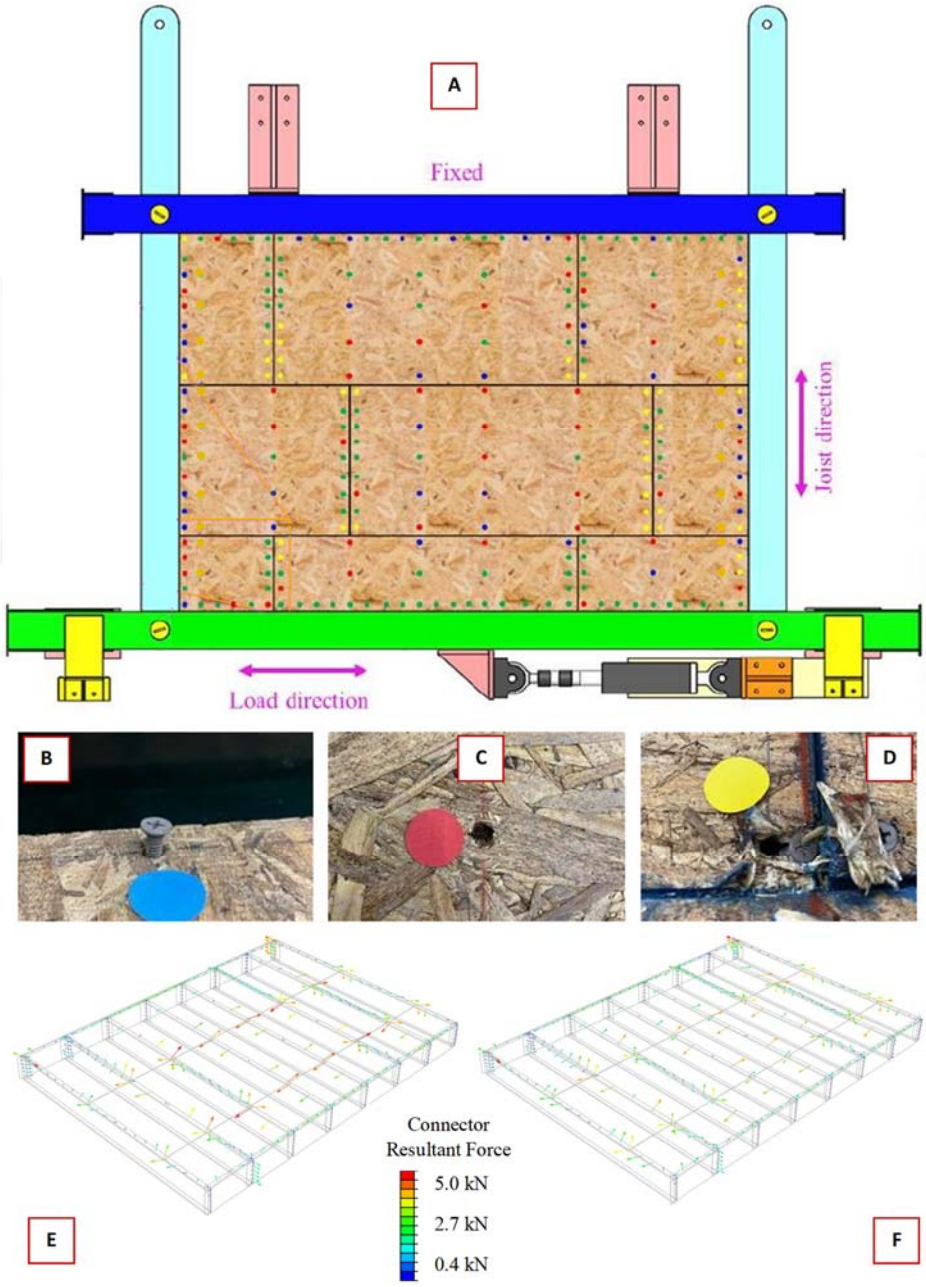

Figure 7: Connection failure of the diaphragm sheathed with OSBs: (A) Failure modes of the OSB-CFS frame connections – (B) Screw pull-out – (C) Screw pull-through – (D) OSB edge tear-out – (E) Connector resultant force at Peak – (F) Connector resultant force post peak

A schematic representation illustrating these fastener failure modes for the entire diaphragm sheathed with OSBs based on the experimental test is shown in Fig. 7.A. The numerical model confirms these findings, indicating the failure of the same fasteners at peak. The connector resultant forces of the screws in the computational model at both peak and post-peak stages are shown in Fig. 7.E and 7.F respectively.
A decrease in the connector resultant forces at the post-peak stage indicates the failure of screws at peak.

6. Conclusions

This paper develops a three-dimensional shell model of a cold-formed steel (CFS) diaphragm sheathed with oriented strand boards. The model aims to capture the stability response, shear strength and connection failure of the system. The outcome of the finite element model is compared to the response of the CFS diaphragm tested experimentally at the University of Massachusetts Amherst. The shear strength and displacement at peak load of the OSB-sheathed diaphragm align closely with the experimental results and the AISI S400 recommended value. Both the numerical and experimental models exhibit identical stability responses, local lip buckling and lateral torsional buckling of the joists of the frame. Both the experimental and computational models observe a separation of the OSBs and reveal failure at the same connections, further elucidating the complex load transfer mechanism of the OSB-sheathed CFS diaphragms.

Acknowledgments

The authors would like to thank USG Co., Canam Steel, Super Stud and ClarkDietrich Corporations for their in-kind support through the donation of the specimen materials. The assistance and guidance provided by the lab technician at UMass Amherst, Mr. Mark Gauthier, is highly appreciated.

References

American Iron and Steel Institute (AISI S400). (2015). *North American standard for the design of cold-formed steel structural members*.

American Iron and Steel Institute (AISI S907). (2017). *Test standard for determining the strength and stiffness of cold-formed steel diaphragms by the cantilever test method*.

Ariana, S., Castaneda, H., & Peterman, K. D. (2023, April). *Progression of failure in cold-formed steel diaphragms sheathed with steel deck*. https://cloud.aisc.org/SSRC/2023/Ariana_et_al_SSRC_2023.pdf

Ariana, S., & Peterman, K. (2023). *Impact of Edge Distance on Hysteretic Behavior of Fiber-Cement-Board Cold-Formed Steel Connections*. https://scholarworks.umass.edu/cee_sem_research_reports

Ariana, S., & Peterman, K. D. (2022, October). *Cyclic performance of fiber-cement-board cold-formed steel connections with varying edge distance*. https://jscholarship.library.jhu.edu/bitstream/handle/1774.2/67701/ID64_Sheila%20Ariana.pdf?sequence=1

Blais, C. (2007). *Testing and analysis of light gauge steel frame/9 mm OSB wood panel shear walls*. Library and Archives Canada = Bibliothèque et Archives Canada.

Boudreault, F. A., Blais, C., & Rogers, C. A. (2007). Seismic force modification factors for light-gauge steel-frame - Wood structural panel shear walls. *Canadian Journal of Civil Engineering*, *34*(1), 56–65. https://doi.org/10.1139/L06-097

Branston, A. E., Boudreault, F. A., Chen, C. Y., & Rogers, C. A. (2006). Light-gauge steel-frame - Wood structural panel shear wall design method. *Canadian Journal of Civil Engineering*, *33*(7), 872–889. https://doi.org/10.1139/L06-036

Bryan Folz, B., & Filiatrault, A. (2001). CYCLIC ANALYSIS OF WOOD SHEAR WALLS. In *JOURNAL OF STRUCTURAL ENGINEERING*.

Buonopane, S. G., Bian, G., Tun, T. H., & Schafer, B. W. (2015). Computationally efficient fastener-based models of cold-formed steel shear walls with wood sheathing. *Journal of Constructional Steel Research*, *110*, 137–148. https://doi.org/10.1016/j.jcsr.2015.03.008

Chatterjee, A., Tomasetti, T., Moen, C. D., Chatterjee, A., Rogers, C. A., & Moen, C. D. (2017). *HIGH FIDELITY MONOTONIC AND CYCLIC SIMULATION OF A WOOD-SHEATHED COLD-FORMED STEEL FRAMED FLOOR DIAPHRAGM*. https://www.researchgate.net/publication/324744274

Dassault System Simulia Corporation. (2014). *ABAQUS/CAE Documentation, Version 6.14-4*. www.simulia.com.

Filiatrault, A., Asce, M., & Folz, B. (2002). Performance-Based Seismic Design of Wood Framed Buildings. *Journal of Structural Engineering* , *128*(1), 39–47. https://doi.org/10.1061/ASCE0733-94452002128:139

Fülöp, L. A., & Dubina, D. (2004). Performance of wall-stud cold-formed shear panels under monotonic and cyclic loading - Part II: Numerical modelling and performance analysis. *Thin-Walled Structures*, *42*(2), 339–349. https://doi.org/10.1016/S0263-8231(03)00064-8

Hein Tun, T. (2014). *Fastener-Based Computational Models of Cold-Formed Steel Shear Walls*. https://digitalcommons.bucknell.edu/honors_theses/249

Mohebbi, S., Mirghaderi, S. R., Farahbod, F., Bagheri Sabbagh, A., & Torabian, S. (2016). Experiments on seismic behaviour of steel sheathed cold-formed steel shear walls cladded by gypsum and fiber cement boards. *Thin-Walled Structures*, *104*, 238–247. https://doi.org/10.1016/j.tws.2016.03.015

Morgan, K. A., Sorhouet, M. A., & Serrette, R. (2002). *Performance of Cold-formed Steel-framed Shear Walls: Alternative Configurations*. https://scholarsmine.mst.edu/ccfss-aisi-spec/48

Nguyen, H., Georgi, H., & Serrette, R. (1996). *Shear Wall Values for Light Weight Steel Framing*. https://scholarsmine.mst.edu/ccfss-aisi-spechttps://scholarsmine.mst.edu/ccfss-aisi-spec/46

Nikolaidou, V., & Latreille, P. (2016). *Characterization of CFS Framed D iaphragm Behaviour American Iron and Steel Institute*.

Peterman, K. D., Stehman, M. J. J., Madsen, R. L., Buonopane, S. G., Nakata, N., & Schafer, B. W. (2016). Experimental Seismic Response of a Full-Scale Cold-Formed Steel-Framed Building. II: Subsystem-Level Response. *Journal of Structural Engineering*, *142*(12). https://doi.org/10.1061/(asce)st.1943-541x.0001578

Reynaud Serrette, Jose Encalada, Georgi Hall, & Brandon Matchen. (2007). *Additional Shear Wall Values for Light Weight Steel Framing*. https://scholarsmine.mst.edu/cgi/viewcontent.cgi?article=1117&context=ccfss-aisi-spec

Schafer, B. W., Li, Z., & Moen, C. D. (2010). Computational modeling of cold-formed steel. *Thin-Walled Structures*, *48*(10–11), 752–762. https://doi.org/10.1016/j.tws.2010.04.008

Tao, F., & Moen, C. (2017). *Monotonic and Cyclic Response of Single Shear Cold-Formed Steel-to-Steel and Sheathing-to-Steel Connections Monotonic and Cyclic Response of Single Shear Cold-Formed Steel-to-Steel and Sheathing-to-Steel Connections*.

Yu, C. (2010). Shear resistance of cold-formed steel framed shear walls with 0.686 mm, 0.762 mm, and 0.838 mm steel sheet sheathing. *Engineering Structures*, *32*(6), 1522–1529. https://doi.org/10.1016/j.engstruct.2010.01.029

Zhang, S., & Xu, L. (2018). Determination of equivalent rigidities of cold-formed steel floor systems for vibration analysis, Part I: Theory. *Thin-Walled Structures*, *132*, 25–35. https://doi.org/10.1016/j.tws.2018.08.001

Zhang, W., Mahdavian, M., Li, Y., & Yu, C. (2017). Experiments and Simulations of Cold-Formed Steel Wall Assemblies Using Corrugated Steel Sheathing Subjected to Shear and Gravity Loads. *Journal of Structural Engineering*, *143*(3). https://doi.org/10.1061/(asce)st.1943-541x.0001681

Zhao, Y. (2004). *Cyclic performance of cold-formed steel stud shear walls.* National Library of Canada = Bibliothèque nationale du Canada.